Introducing asymmetric functionality to MOFs via generation of metallic Janus MOF particles†

Received 00th January 20xx,
Accepted 00th January 20xx

DOI: 10.1039/x0xx00000x

www.rsc.org/

Abraham Ayala,[a] Carlos Carbonell,[a] Inhar Imaz, *[a] and Daniel Maspoch *[ab]

Herein we report a versatile methodology for engineering metallic Janus MOF particles based on desymmetrization at interfaces, whereby each MOF particle is partially coated with a desired metal. We demonstrate that it enables fabrication of homogeneous Janus MOF particles according to the MOF (ZIF-8, UiO-66 or UiO-66-SH), the metal (Au, Co or Pt), the MOF particle size (from the micrometer to the submicrometer regime) and the metal-film thickness (from 5 nm to 50 nm) employed. We anticipate that our strategy could be applied to impart new functionalities to MOFs, including asymmetric functionalization, magnetic-guidance and motorization.

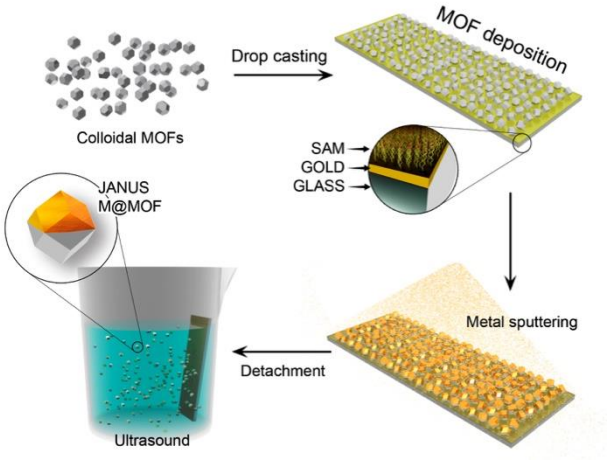

Scheme 1. Synthesis of metallic Janus MOF particles via the desymmetrization at interfaces approach.

Janus particles are a type of multicompartmental, asymmetric particles whose surface has two chemically distinct regions.[1-5] Their dual surface composition has recently attracted growing interest because it can be exploited to confer a single particle with different properties (*e.g.* anisotropy and directionality). For example, Janus design enables combination of two opposing properties, hydrophobicity and hydrophilicity, into single particles that can be used to build water repellent membranes,[6] emulsifiers[7] and Pickering emulsions.[8] In this context, the introduction of porosity into such particles has become a powerful tool to provide porous materials with new functionalities (*e.g.* magnetism,[9] mobility,[10, 11] etc.) and therefore, to enhance their performance in numerous applications such as in biomedicine, catalysis, pollutant removal, and sensors. For example, Sánchez *et al.* have demonstrated that hollow mesoporous MCM-41 particles capable of transporting and delivering drugs can be motorized by functionalizing half of their surface with enzymes.[11] Also, Pingarrón *et al.* have shown that Janus particles comprising Au and mesoporous silica could be used in electrochemical biosensing systems.[12]

Among the various porous materials available, metal-organic frameworks (MOFs) and porous coordination polymers (PCPs) are attractive choices for making porous Janus particles.[13-15] MOFs are attainable in various pore sizes and shapes and with extremely large surface areas, tailored internal surfaces and high flexibility, making them potentially useful for myriad applications, including gas storage, separation, catalysis, molecular sensing, adsorption for heat-pump processes, contaminant removal, contrast agents, and drug delivery systems.[16-18] Seeking to impart MOFs with new functionalities, researchers have recently begun to combine these particles with other functional materials (mainly, inorganic nanoparticles).[19,20] Most of the resulting MOF-based composites are isotropic core-shell materials in which the metallic component is embedded within the MOF. These composites have shown important advantages in some of the afore-mentioned applications, but their isotropicity prevents their use in applications that require anisotropic MOF-metal composites. Importantly, Bradshaw, Kuhn *et al.* have recently demonstrated the synthesis of metallic Janus MOF materials by electrochemically growing ZIF-8 and HKUST-1 crystals in selected regions of macroscopic Zn wires and Cu beads.[21] Also, Lahann *et al.* have shown the spatioselective growth of HKUST-1 nanocrystals on micrometer polymer spheres.[22] However, to date, no suitable methods for forming submicron-sized metallic Janus particles comprising single MOF particles have been described.

[a] *Catalan Institute of Nanoscience and Nanotechnology (ICN2), CSIC and The Barcelona Institute of Science and Technology, Campus UAB, Bellaterra, 08193 Barcelona, Spain.*
[b] *Institució Catalana de Recerca i Estudis Avançats (ICREA) 08100 Barcelona (Spain)*

†Electronic Supplementary Information (ESI) available. See DOI: 10.1039/x0xx00000x

Herein we report a general strategy to synthesize porous metallic Janus MOF particles, based on direct evaporation of metals on the surface of colloidal MOF crystals that have been pre-immobilized onto planar surfaces. The approach that we used is also known as desymmetrization at interfaces. We have named these Janus particles *M@MOF* particles, in which *M* refers to the evaporated metal and *MOF*, to the selected colloidal MOF.

Desymmetrization at interfaces using planar surfaces has already been used to synthesize metal/polystyrene and metal/silica Janus particles.[23,24] When a metal is evaporated from above onto particles affixed to a planar surface, it is selectively deposited on the top (exposed) surfaces of the particles. Subsequent detachment of the particles from the surface affords Janus particles whose top surfaces are covered by a thin metallic film and whose bottom surfaces (*i.e.* the previously unexposed surfaces that had been in contact with the planar surface) remain unaltered. For the work that we report here, we adapted this method to MOF crystals.

Initially, in a typical experiment, we synthesized colloidal MOF particles of different sizes by adjusting the conditions of previously reported methods.[25-29] The selected MOFs were ZIF-8 (particle sizes = 101 ± 10 nm, 201 ± 9 nm, and 1.3 ± 0.2 µm; S_{BET} = 1272 m^2/g, 1123 m^2/g and 1272 m^2/g, respectively); UiO-66 (particle size = 190 ± 22 nm; S_{BET} = 1332 m^2/g) and UiO-66-SH (particle size = 208 ± 54 nm; S_{BET} = 306 m^2/g) (Fig. S1-S6, ESI†). Each MOF was then deposited onto Au surfaces that had been pre-functionalized with 4-mercaptobenzoic acid and treated with NaOH to deprotonate the carboxylic groups (Fig. S7, ESI†). For the deposition, a colloidal MOF solution in DMF was spread onto the surface, which was then heated at 60 °C until the DMF had evaporated off. Here, we made a strategic decision to carefully cover the surface with a true monolayer (even though some areas remained uncovered) rather than to fully cover the surface and risk forming MOF aggregates or multilayers, as any MOF particles underneath the resultant top layer would not be covered in the subsequent next stage. In a third step, the surface-deposited MOF particles were coated with a metal (M = Au, Co or Pt; metal film thickness = 5 nm to 50 nm) using an E-beam evaporator. Finally, the resultant Janus M@MOF particles were detached by ultrasonication of the surfaces for 30 s in MeOH. The particles were characterized by Scanning Electron Microscopy (SEM), and their corresponding porosity capabilities were evaluated.

Next, to confirm the generality of our approach, we systematically studied the formation of diverse Janus Au@MOF particles that varied by MOF (ZIF-8 and UiO-66), particle size (particle sizes = 101 ± 10 nm, 201 ± 9 nm, and 1.3 ± 0.2 µm for ZIF-8 and 190 ± 22 nm for UiO-66) and Au film thickness (5 nm, 10 nm, 20 nm, 30 nm or 50 nm). SEM images of all synthesized Janus particles revealed the partial coverage of the external surface of the MOF with an Au thin film (Fig. 1a-e and Fig. S8-S11, ESI†). The asymmetric structure of these particles was further confirmed by elemental mapping with energy dispersive X-ray spectrometry (EDX) of single particles, which revealed a uniform distribution of Au atoms in approximately half of the particle surface (Fig. 1f and Fig. S12, ESI†). Additionally, SEM images confirmed that the Au film thickness on the Janus particles could be easily controlled with this method. This thickness increase was further corroborated by EDX analyses, which indicated that the Au:Zn or Au:Zr ratio consistently increased with increasing Au film thickness (Fig. S8-S11, ESI†).

One might expect that the many synthetic steps required for the Janus particles would affect the initial crystalline integrity and adsorption capabilities of the MOFs; however, we did not observe any losses in these properties. Indeed, for all Janus particles, the simulated (derived from the single crystal structure) and experimental X-ray powder diffraction (XRPD) patterns were consistent (Fig. S13-S16, ESI†), confirming that the ZIF-8 or UiO-66 in the Janus particles were structurally identical to corresponding starting MOF particles. As expected, characteristic peaks for crystalline Au were also observed. Additionally, N_2 sorption measurements taken at 77 K up to 1 bar of Au@ZIF-8 (ZIF-8 size = 201 ± 9 nm; Au film thickness = 50 nm) and Au@UiO-66 (Au film thickness = 5 nm) particles proved that the sorption capacity of these particles was equivalent to that of the initial MOF particles (Fig. S17,S18, ESI†). Thus, the S_{BET} values were determined to be 456 m^2/g for Au@ZIF-8 and 560 m^2/g for Au@UiO-66. Given that Au thin film is non-porous to N_2, we attributed the sorption exclusively to ZIF-8 or UiO-66. Therefore, these S_{BET} values could be expressed in m^2 per grams ZIF-8 (S_{BET} = 1037 m^2/g) or UiO-66 (S_{BET} = 982 m^2/g),

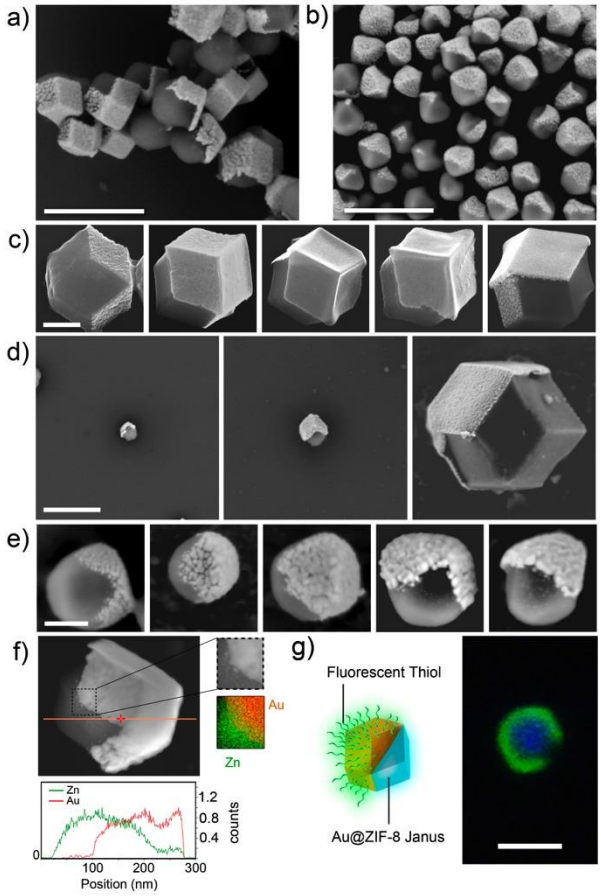

Fig. 1. (a,b) Representative FESEM images showing a general view of (a) Au@ZIF-8 particles (size = 201 ± 9 nm; Au thickness = 50 nm) and (b) Au@UiO-66 particles (size = 190 ± 22 nm; Au thickness = 50 nm). (c) FESEM images of individual Au@ZIF-8 particles (size = 1.3 µm ± 0.2 µm), showing different Au thicknesses (from left to right: 5 nm, 10 nm, 20 nm, 30 nm and 50 nm). (d) FESEM images of individual Au@ZIF-8 particles (Au thickness = 50 nm), showing different ZIF-8 sizes (from left to right: 101 ± 10 nm, 201 ± 9 nm and 1.3 µm ± 0.2 µm). (e) FESEM images of individual Au@UiO-66 particles (size = 190 ± 22 nm), showing different Au thicknesses (from left to right: 5 nm, 10 nm, 20 nm, 30 nm and 50 nm). (f) EDX mapping of a single Au@ZIF-8 particle (size = 201 µm ± 9 nm), showing the distribution of Zn (green) and Au (red). g) Schematic illustration and corresponding confocal image (ZIF-8, blue; FITC-PEG-SH, green), showing the asymmetric functionalization of a single Au@ZIF-8 particle (size = 1.3 µm ± 0.2 µm). Scale bars: 500 nm (a-d), 100 nm (e) and 1.5 µm (g).

once had we calculated the amount of Au present in each samples (56% w/w for Au@ZIF-8; 43% w/w for Au@UiO-66). The latter step was completed upon selectively dissolving the MOF component using an aqueous HCl solution (pH < 1) for ZIF-8 and an aqueous H_2SO_4 solution (pH < 1) for UiO-66. From the calculated S_{BET} values, we found that the sorption performance of both MOFs in the Janus particles remains unaltered.

As proof-of-concept of the properties that metallic Janus MOF particles can incorporate, we explored asymmetric functionalization of them. To this end, we selectively attached the green fluorophore fluorescein isothiocyanate polyethylene glycol thiol (FITC-PEG-SH) onto the Au thin film. The asymmetric functionalization was performed by incubating Au@ZIF-8 particles in an aqueous solution of FITC-PEG-SH at 4 ^{o}C for 24 h. The resulting FITC-PEG-S-Au@ZIF-8 particles were then collected by centrifugation, cleaned twice with methanol, and imaged by confocal laser scanning microscopy (Fig. 1g and Fig. S19, ESI†). The results clearly show two different fluorescent regions corresponding to ZIF-8 (blue)[30] and to FITC-PEG-SH (green) that is selectively attached to the Au surfaces. Our successful demonstration of asymmetric functionalization of metallic Janus MOF particles suggests that in the future, such particles could be vectorized for biomedical and sensing applications. Furthermore, our approach could be advantageous modulating certain properties (*e.g.* hydrophobicity, hydrophilicity) of the base MOF without altering its porosity.

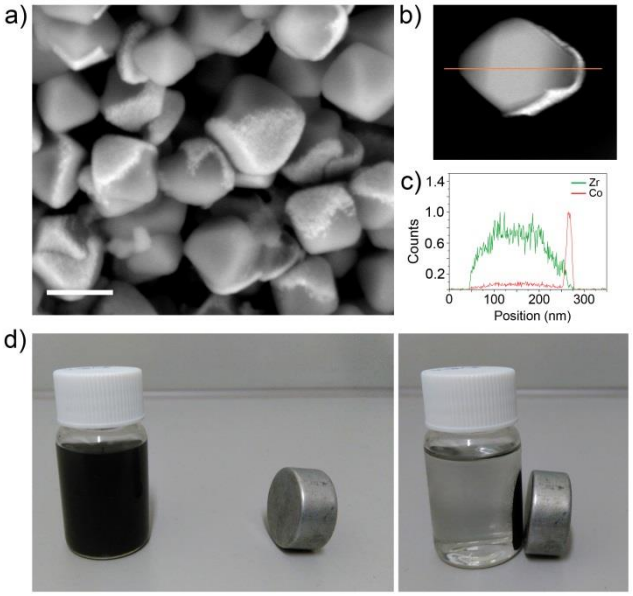

Fig. 2. (a) Representative FESEM images of Co@UiO-66-SH (Co film thickness = 20 nm). (b) EDX mapping of a single Co@UiO-66-SH particle showing the Zr (green) and Co (red) distribution. (d) Photographs showing the magnetic attraction of Co@UiO-66-SH particles dispersed in an aqueous solution of mercury before (left) and during (right) exposure to a magnet. Scale bars: 500 nm (a).

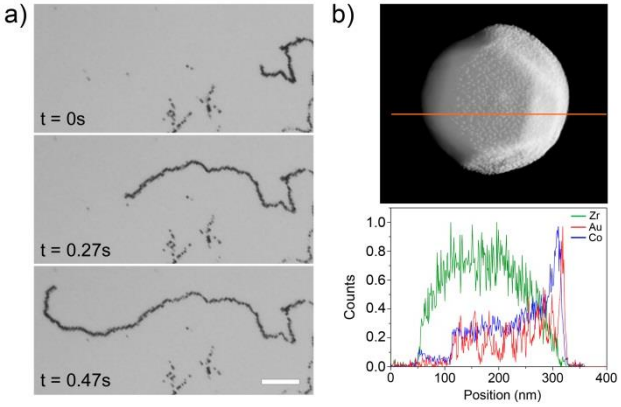

Fig. 3. (a) Optical microscopy images revealing the movement sequence of a motorized Pt@ZIF-8 particle. Scale bar: 100 µm. (b) EDX mapping of a single Au@Co@UiO-66 particle, showing the Zr (green), Co (blue) and Au (red) distributions.

We next sought to create magnetically guidable porous particles. To this end, we synthesized Janus particles as above, except that we replaced Au with Co in order to confer the particles with magnetism. Figures 2a, S20 and S21 show the resultant Janus Co@ZIF-8, Co@UiO-66 and Co@UiO-66-SH particles (size = *ca*. 200 nm; Co film thickness = 20 nm). In all cases, EDX and XRPD analyses confirmed the desired asymmetric structure (Fig. 2b,c), the presence of crystalline Co, and that the crystalline integrity of all three MOFs had been fully conserved (Fig. S22-24, ESI†). More importantly, all the Janus particles incorporated the magnetic properties of the Co component, as demonstrated by the fact they could be easily guided by a magnet (Fig. 2d). Magnetic measurements also confirmed the magnetism of the particles, which exhibit a characteristic hysteresis loop with coercive field values of 181 Oe (Co@ZIF-8), 350 Oe (Co@UiO-66) and 23 Oe (Co@UiO-66-SH) at room temperature (Fig. S25, ESI†).

To demonstrate that these Janus particles could be employed to adsorb target substances and subsequently magnetically recovered, we tested the performance of Co@UiO-66-SH particles in magnetic solid-phase removal of mercury. To this end, Co@UiO-66-SH particles (2 mg) were dispersed in a solution of 10 ppm Hg^{2+} in water (4 mL) at room temperature. After 30 min of incubation, the mercury content adsorbed by the Janus particles was determined by ICP-MS. The observed extraction was highly efficient: the particles had sequestered 99% of the mercury from the solution,[29] and could then be easily removed using a small magnet (Fig. 2d).

Once we had demonstrated that MOF particles could be asymmetrically metallized, we then sought to explore development of motorized MOFs powered by electrochemistry, using Pt as the metal.[14, 31] To this end, we fabricated Janus Pt@ZIF-8 particles (ZIF-8 size = 1.3 ± 0.2 µm, or ~ 8 µm for better visualization under optical microscopy; Pt film thickness = 60 nm; Fig. S26,27, ESI†), and then dropped them onto the surface of an aqueous/ethanol solution containing sodium cholate and H_2O_2. The Pt@ZIF-8 moved, and their motion was recorded using an optical microscopy. As shown in Figure 3a (see also Video S1,2), the 8 µm-in-diameter particles behaved as motors, moving around the surface at a maximum speed of 1.65 mm·s^{-1} (measured by ImageJ software using 20 frames).

Finally, we tested our method for fabrication of polymetallic Janus MOF particles, which we made by sequentially evaporating different metals on the surface of the colloidal MOF crystals. Thus, UiO-66 crystals were first coated with Co (thickness = 20 nm) and

then, with Au (thickness = 5 nm). The resulting particles were confirmed by XRPD and EDX elemental mapping to be polymetallic Au@Co@UiO-66 particles (Fig. 3b and Fig. S28, ESI†). Interestingly, these Janus particles marry the porosity capabilities of UiO-66, the magnetic properties of Co and the easy chemical functionalization of the external Au layer (Fig. S25,S29, ESI†).

In conclusion, we have described a collection of monometallic and polymetallic Janus MOF particles fabricated by partially coating colloidal MOF crystals with the desired metal(s). We consider this approach a novel method for imparting new functionalities to MOFs, as evidenced by our preparation of asymmetrically functionalized MOFs, magnetically guidable MOFs and electrochemically motorized MOFs. Our findings should facilitate development of MOFs for numerous practical applications, including drug delivery, theranostics, sensors, pollutant removals and catalysis.

This work was supported by the MINECO-Spain through projects PN MAT2012-30994 and EU FP7 ERC-Co 615954. I.I. thanks the MINECO for a RyC, and A.A. is grateful to the CONACYT for a predoctoral grant. ICN2 acknowledges the support of the Spanish MINECO through the Severo Ochoa Centers of Excellence Program, under Grant SEV-2013-0295.

Notes and references

1. A. Walther and A. H. E. Müller, *Chem. Rev.*, 2013, **113**, 5194-5261.
2. A. Walther and A. H. E. Muller, *Soft Matter*, 2008, **4**, 663-668.
3. A. Perro, S. Reculusa, S. Ravaine, E. Bourgeat-Lami and E. Duguet, *J. Mater. Chem.*, 2005, **15**, 3745.
4. K.-H. Roh, D. C. Martin and J. Lahann, *Nat. Mater.*, 2005, **4**, 759-763.
5. S. Jiang, Q. Chen, M. Tripathy, E. Luijten, K. S. Schweizer and S. Granick, *Adv. Mater.*, 2010, **22**, 1060-1071.
6. F. Liang, K. Shen, X. Qu, C. Zhang, Q. Wang, J. Li, J. Liu and Z. Yang, *Angew. Chem. Int. Ed.*, 2011, **50**, 2379-2382.
7. S. Fujii, Y. Yokoyama, Y. Miyanari, T. Shiono, M. Ito, S.-i. Yusa and Y. Nakamura, *Langmuir*, 2013, **29**, 5457-5465.
8. Y. Huang, S. Xu and V. S. Y. Lin, *Angew. Chem. Int. Ed.*, 2011, **50**, 661-664.
9. Y. Qu, J. Bai, L. Liao, R. Cheng, Y.-C. Lin, Y. Huang, T. Guo and X. Duan, *Chem. Commun.*, 2011, **47**, 1255-1257.
10. X. Ma, A. Jannasch, U.-R. Albrecht, K. Hahn, A. Miguel-López, E. Schäffer and S. Sánchez, *Nano Lett.*, 2015, **15**, 7043-7050.
11. X. Ma, K. Hahn and S. Sanchez, *J. Am. Chem. Soc.*, 2015, **137**, 4976-4979.
12. A. Sánchez, P. Díez, P. Martínez-Ruíz, R. Villalonga and J. M. Pingarrón, *Electrochem. Commun.*, 2013, **30**, 51-54.
13. M. Meilikhov, S. Furukawa, K. Hirai, R. A. Fischer and S. Kitagawa, *Angew. Chem.*, 2013, **125**, 359-363.
14. T. T. Tan, J. T. Cham, M. R. Reithofer, T. S. Hor and J. M. Chin, *Chem. Commun.*, 2014, **50**, 15175-15178.
15. P. A. Szilagyi, M. Lutz, J. Gascon, J. Juan-Alcaniz, J. van Esch, F. Kapteijn, H. Geerlings, B. Dam and R. van de Krol, *CrystEngComm*, 2013, **15**, 6003-6008.
16. Special issue on metal-organic framework materials. Chem. Soc. Rev., 2014, **43**, 5415.
17. Special issue on metal organic framework materials. *Chem. Soc. Rev.*, 2009, **38**, 1201.
18. B. Seone, S. Castellanos, A. Dikhtiarenko, F. Kapteijn, J. Gascon, *Coord. Chem. Rev.*, 2016, **307**, 147.
19. P. Falcaro, R. Ricco, A. Yazdi, I. Imaz, S. Furukawa, D. Maspoch, R. Ameloot, J. D. Evans and C. J. Doonan, *Coord. Chem. Rev.*, 2016, **307**, 237-254.
20. G. Lu, S. Li, Z. Guo, O. K. Farha, B. G. Hauser, X. Qi, Y. Wang, X. Wang, S. Han, X. Liu, J. S. DuChene, H. Zhang, Q. Zhang, X. Chen, J. Ma, S. C. J. Loo, W. D. Wei, Y. Yang, J. T. Hupp and F. Huo, *Nat. Chem.*, 2012, **4**, 310-316.
21. S. Yadnum, J. Roche, E. Lebraud, P. Négrier, P. Garrigue, D. Bradshaw, C. Warakulwit, J. Limtrakul and A. Kuhn, *Angew. Chem. Int. Ed.*, 2014, **53**, 4001-4005.
22. T.-H. Park, K. J. Lee, S. Hwang, J. Yoon, C. Woell, J. Lahann, *Adv. Mater.*, 2014, **26**, 2883.
23. J. Choi, Y. Zhao, D. Zhang, S. Chien and Y. H. Lo, *Nano Lett.*, 2003, **3**, 995-1000.
24. S. Ye and R. L. Carroll, *ACS Appl. Mater. Interfaces*, 2010, **2**, 616-620.
25. J. Cravillon, R. Nayuk, S. Springer, A. Feldhoff, K. Huber and M. Wiebcke, *Chem. Mater.*, 2011, **23**, 2130-2141.
26. L. Chen, Y. Peng, H. Wang, Z. Gu and C. Duan, *Chem. Commun.*, 2014, **50**, 8651-8654.
27. J. Cravillon, C. A. Schroder, H. Bux, A. Rothkirch, J. Caro and M. Wiebcke, *CrystEngComm*, 2012, **14**, 492-498.
28. G. Lu, C. Cui, W. Zhang, Y. Liu and F. Huo, *Chem. Asian J.*, 2013, **8**, 69-72.
29. K.-K. Yee, N. Reimer, J. Liu, S.-Y. Cheng, S.-M. Yiu, J. Weber, N. Stock and Z. Xu, *J. Am. Chem. Soc.*, 2013, **135**, 7795-7798.
30. S. Liu, Z. Xiang, Z. Hu, X. Zheng and D. Cao, *J. Mater. Chem.*, 2011, **21**, 6649-6653.
31. Y. Ikezoe, G. Washino, T. Uemura, S. Kitagawa and H. Matsui, *Nat. Mater.*, 2012, **11**, 1081-1085.